Magnetic Anisotropy and Spin Parity Effect Along the Series of Lanthanide Complexes with DOTA**

*Marie-Emmanuelle Boulon, Giuseppe Cucinotta, Javier Luzon, Chiara Degl'Innocenti, Mauro Perfetti, Kevin Bernot, Guillaume Calvez, Andrea Caneschi, and Roberta Sessoli**

Magnetic anisotropy, arising from the unquenched orbital contribution of the partially occupied inner 4f orbital combined with the crystal field that breaks the spherical symmetry, is the key property that makes lanthanides a unique ingredient in magnetism. Molecular magnetism makes no exception, especially in the field of bistable materials, like single-molecule magnets (SMM)[1,2] and single-chain magnets (SCM).[3,4] In the first case the magnetic anisotropy generates a barrier for the reversal of the magnetization of the molecule that can be overcome either by thermal activation, leading to an exponential growth of the relaxation time at low temperature, or by underbarrier mechanisms, which are severely affected by the symmetry of the crystal field and by the application of an external magnetic field.[2]

After the discovery of SMM behavior in a mononuclear Tb sandwich complex with phthalocyaninato ligand[5] an intense research activity has been focused on the design of high-symmetry environments for single lanthanide ions, including polyoxometallate[6] and organometallic sandwich complexes,[7,8] with the aim to reduce the efficiency of the tunnel mechanism of magnetic relaxation and to increase the blocking temperature of the material. Magneto-structural correlations based on the distribution of the ligand negative charges around the lanthanide ions rely on the generally accepted assumption that the interaction of the magnetic orbitals with the ligand donor atoms is electrostatic, given the inner character of the 4f electrons.[9,10]

[*] Dr. M.-E. Boulon, G. Cucinotta, C. Degl'Innocenti, M. Perfetti, Prof. Dr. A. Caneschi, Prof. Dr. R. Sessoli
Department of Chemistry "Ugo Schiff" and
INSTM RU University of Florence
50019 Sesto Fiorentino (Italy)
E-mail: roberta.sessoli@unifi.it
Dr. J. Luzon
Centro Universitario de la Defensa and
Instituto de Ciencia de Materiales, AGM
50090 Zaragoza (Spain)
Dr. K. Bernot, Dr. G. Calvez
Université Européenne de Bretagne, INSA, SCR, UMR 6226
35708 Rennes (France)

[**] This work was supported by the European Research Council through the AdG "NoINanoMaS" (grant number 267746), by the Italian MIUR (PRIN 2008), Spanish research project MAT2011-27233-C02-02, Région Bretagne, Rennes Métropole, and by the Italien CINECA through the award number HP10AI85MB, 2011.

Rinehart and Long have recently associated the presence/absence of SMM behavior in complexes of tripositive lanthanides to the combination of the spatial distribution of negative charges of the 4f electrons with that of the ligands donor atoms.[9] The geometry of the 4f orbitals, can be prolate (elongated), oblate (flattened), or spherical. Easy axis, or Ising, magnetic anisotropy, a prerequisite for observing magnetic bistability, is favored when the ligand field stabilizes the state with the largest projection of the total angular momentum, *J*. This occurs for oblate ions with ligands that concentrate the negative charges in an axial position, while equatorial ligands are predicted to favor SMM behavior in prolate ions.

We have recently investigated the magnetic behavior of $Na[DyDOTA(H_2O)]\cdot 4H_2O$, where $DOTA^{4-}$ is the anion of 1,4,7,10-tetraazacyclododecane-1,4,7,10-tetraacetic acid. DOTA-based lanthanide complexes have been widely employed as magnetic resonance imaging contrast agents[11] and luminescent materials[12] but their low-temperature magnetic behavior has remained unexplored until recently, when the Dy^{III} complex revealed to be a SMM with giant field dependence of the relaxation time.[13] Angle-resolved magnetometry gave access to the magnetic anisotropy tensor and surprisingly the easy axis was found to be perpendicular to the pseudo four-fold symmetry axis of the capped square-antiprism coordination environment of the DOTA ligand,[14] as shown in Figure 1 where the easy axis is drawn as a pink rod superimposed to the molecule. This observation has risen questions about the general validity of the assumption on the electrostatic nature of the metal–ligand interaction and possible synthetic strategies we can develop to control the magnetic anisotropy of lanthanide-based materials.[15] To get a deeper insight in this fundamental issue we investigated the magnetic behavior of Tb^{III}, Ho^{III}, Er^{III}, Tm^{III}, and Yb^{III} derivatives with the DOTA ligand, as late lanthanide ions are characterized by larger *J* ground states. We evidenced a progressive rotation in the orientation of the magnetic anisotropy on increasing the number of 4f electrons, as well as the disappearance of SMM behavior when this number is even. Although some experimental and theoretical investigations of isostructural Ln-based systems[16–21] have been reported, the direct comparison between experimental anisotropy tensors and calculated ones for Ln^{III} ions different from Dy^{III} is, to the best of our knowledge, unprecedented.

$Na[LnDOTA(H_2O)]\cdot 4H_2O$, with $Ln^{III} = Tb^{III}$, Ho^{III}, Er^{III}, Tm^{III}, and Yb^{III}, from here on abbreviated with the lanthanide atomic symbol in bold, were obtained following the reported procedure[22] (see SI Table S1). All were found to be isostructural to the Dy^{III} derivative by either checking the

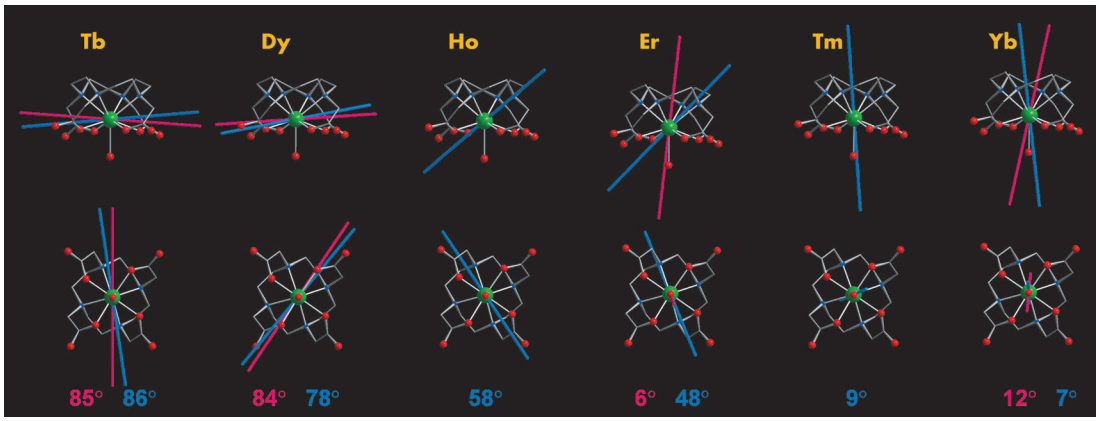

Figure 1. Experimental (pink) and calculated (blue) magnetization easy axis at $T = 2$ K for the series viewed perpendicular (top) and parallel (bottom) to the pseudo four-fold symmetry axis of the molecules. The reported angles are those formed by the easy axes and the Ln–O_w direction (same color code as above). Ln atoms are drawn in green, O in red, N in blue, and C in gray.

crystallographic unit cell through single-crystal diffraction or recording X-ray powder diffraction patterns (Table S2 and Figure S1 in the Supporting Information).

The analysis of their static magnetic properties revealed the typical behavior of tripositive lanthanide ions with orbital contribution (Figures S2 and S3). The temperature dependence of the magnetic susceptibility provided the following Curie constant, 11.74, 14.92, 11.63, 7.46, and 2.30 emu K mol^{-1}, which are in agreement with that expected for $J = L + S$ values of 6, 8, 15/2, 6, and 7/2 with $g_J = 3/2$, 5/4, 6/5, 7/6, and 8/7, which characterize tripositive Tb, Ho, Er, Tm, and Yb ions, respectively. On decreasing the temperature a general decrease of the $\chi_M T$ product is observed because of the depopulation of sublevels of the ground J multiplet split by the crystal field.

In the case of Tb^{III}, Er^{III}, and Yb^{III} derivatives, crystals with the largest dimension approaching 1 mm, and thus suitable for single-crystal magnetic analysis, were obtained (see the Supporting Information). They were mounted on teflon cubes accordingly to a recently developed procedure, and investigated by single-crystal X-ray diffraction to index the faces of the cube in the crystal reference frame of the compound.[23,24] The angular dependence of the magnetic susceptibility was measured by rotating along three orthogonal axes, corresponding to the normal to the faces of the cube. Strong magnetic anisotropy characterizes all compounds (Figures S4–S5, S7–S8, and S10 for **Tb**, **Er**, and **Yb**, respectively). Whereas **Tb** showed an appreciable shift (about 10°) of the position of maxima and minima upon heating from 2 to 10 K, no shift was observed for **Er** and **Yb**, as was the case for **Dy**. The susceptibility tensors, extracted from the angular dependence data (see the Supporting Information for details) gave the following principal values at $T = 2$ K: 10.4, 1.59, and 0.49 emu mol^{-1} for **Tb**; 5.2, 1.7, and 1.2 emu mol^{-1} for **Er** and 1.07, 0.39, and 0.34 emu mol^{-1} for **Yb** (see also Tables S3 to S5). All systems have an easy axis of magnetization with strong rhombic anisotropy. The orientation of the easy axis at $T = 2$ K is shown in Figure 1. At a first glance we can notice that the easy axis is perpendicular to the Ln-O_w bond, that is, perpendicular to the axial direction in the capped square antiprism, for **Tb** (85°) and **Dy** (84°), but is almost parallel to this bond for **Er** (6°) and **Yb** (12°); the experimental error of the procedure is evaluated not to exceed 10°. The results clearly show the importance of matching the ligand geometry with the electron density distribution of the lanthanide ion.

For **Tb** and **Er** single crystals the magnetic signal was strong enough to allow measuring the field dependence of the magnetization at different temperatures. The curves, reported as Figures S6 and S9 revealed a nonperfect superposition when plotted versus the rescaled variable H/T. Anyhow, the analysis with the Brillouin function with $S_{eff} = 1/2$ provided a best fit for $g = 14.2$ and 7.8 for **Tb** and **Er**, respectively.

Quantum chemistry calculation based on the relativistic quantum chemistry method CASSCF/CASPT2-RASSI-SO approach as implemented in the MOLCAS 7.4 code[25] have demonstrated to be a precious tool to rationalize the magnetic behavior of lanthanide-based molecular clusters and chains.[26–33] In the case of **Dy** we have previously evidenced that the magnetic anisotropy is strongly sensitive to minor structural details, like the orientation of the H-O-H plane of the apical coordinated water.[14] We therefore extended the calculation to the whole investigated series, employing a similar cluster model to take into account the triclinic environment of the complex (see the Supporting Information for details and Figure S11). The results are gathered in Figure 1, where the calculated easy axis of magnetization is drawn as a blue rod. In Table 1 the energy levels of the ground J multiplet and the principal values of the extracted gyromagnetic tensor, assuming an effective $S_{eff} = 1/2$, are reported (see also Figure S12). While for Kramers ions (odd number of electrons) the calculation of the g tensor is straightforward, in the case of non-Kramers ions, anisotropy axes, and gyromagnetic factors have been extracted from the diagonalization of the susceptibility matrix tensor at $T = 2$ K.

In Figure 1 we notice a gradual rotation of the easy axis from orthogonal towards parallel to the M–O_w bond (see the angle values in blue) on increasing the number of 4f electrons. We can also notice that the agreement between calculated and observed anisotropy is good except for **Er**, for which the easy axis is calculated in an intermediate position while exper-

Table 1: Gyromagnetic factors along the main anisotropy axes and energy level structure of the ground $^{2S+1}L_J$ multiplet from the relativistic ab initio calculations. For non-Kramers ions gyromagnetic factors have been computed at $T = 2$ K.

Gyromagnetic factors along the main anisotropy axes						
	g_1		g_2		g_3	
Tb	12.7		2.1		0.5	
Ho	6.2		3.3		1.3	
Er	10.9		2.8		1.8	
Tm	12.02		1.02		0.95	
Yb	6.8		1.0		0.1	
Ground-state multiplet energy levels [cm^{-1}]						
Tb	Singlets:	0.0	1.6	25.4	29.8	115.6
	144.0	159.9	213.7	245.9	314.4	323.9
	379.9	384.4				
Ho	Singlets:	0.0	4.8	29.9	44.1	87.5
	145.8	155.6	172.2	185.5	192.9	214.0
	227.5	253.6	273.4	290.5	303.8	309.2
Er	Doublets:	0.0	19.8	63.2	77.1	163.2
	228.8	317.5	427.0			
Tm	Singlets:	0.0	4.6	99.0	105.3	143.0
	173.0	206.6	225.5	260.6	307.5	325.5
	384.2	384.7				
Yb	Doublets:	0.0	197.2	379.3	416.2	

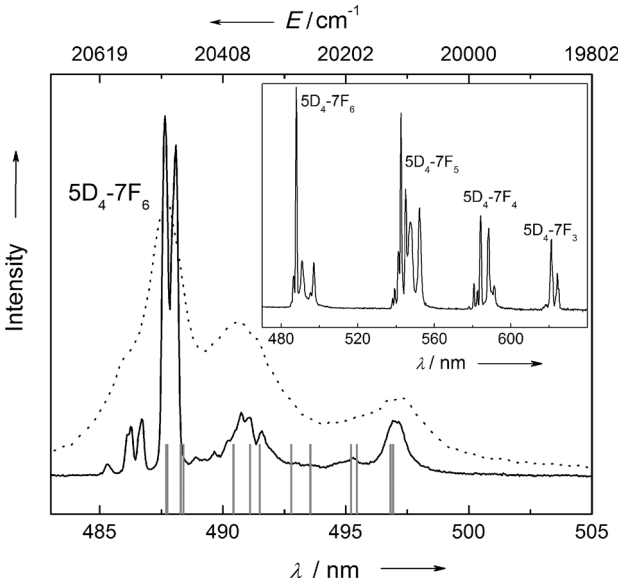

Figure 2. Luminescence spectrum in the region involving the $^5D_4 \rightarrow {}^7F_6$ transition of a polycrystalline powder sample of **Tb** excited at 380 nm at room temperature (dotted line) and at 77 K (solid line). The calculated energy levels of the $^7F_6$ multiplet are represented by gray bars. Inset: full emission spectra in the 450 to 680 nm range.

imentally it lies along the M-O_w bond. It must be noted that **Er** is the only derivative showing in the ab initio calculations a large influence of the dynamic electronic correlation correction (CASPT2).[34] This fact makes the accurate determination of the direction of the easy anisotropy axis more complex.

As far as **Tb** is concerned, we notice that the separation between the first excited state and the ground state is 1.6 cm^{-1}, which could justify the change in the magnetic anisotropy on increasing the temperature from 2 to 10 K.[19] Another interesting feature is that the easy axis of magnetization is at about 45° from the normal to the H-O-H plane of the apical water molecule, while it was at about 90° for the Dy^{III} derivative.

To further check the validity of our ab initio calculations we have exploited the efficient luminescence in the visible range that characterizes Tb^{III}. The luminescence spectrum of **Tb** was recorded at room temperature and at 77 K on a polycrystalline powder (Figure 2 and Figures S13–14) with the excitation wavelength of 380 nm. Well resolved multiline emissions were observed and attributed as $^5D_4 \rightarrow {}^7F_6$ (28500 cm^{-1}), $^5D_4 \rightarrow {}^7F_5$ (18500 cm^{-1}), $^5D_4 \rightarrow {}^7F_4$ (17000 cm^{-1}), and $^5D_4 \rightarrow {}^7F_3$ (16000 cm^{-1}) transitions. A quantum yield of 34%, significantly larger than for the Dy^{III} derivative, was observed and the room-temperature lifetime was evaluated to be 1.68 ms.

In Figure 2 the spectral region involving transitions to the ground multiplet $J = 6$ and the calculated energy levels from ab initio calculation are shown. The temperature dependence suggests that all features above the intense one at 20530 cm^{-1} are hot transitions, that is, coming from an excited state of the $^5D_4$ multiplet. Rescaling the ground-state energy to the emission at 20530 cm^{-1} the overall separation of the $^7F_6$ manifold is well reproduced.

Given the easy axis anisotropy of the entire series we also investigated the magnetization dynamics by alternating current (ac) susceptometry (see Figures S15 to S19). In static zero field all compounds, except **Dy**, did not reveal a significant out of phase, χ'', component of the susceptibility.

Applying a magnetic static field well-resolved maxima in the frequency dependence of χ'' were observed for **Er** and **Yb**, but interestingly no out-of-phase susceptibility was detected for **Tb**, **Ho**, and **Tm**. As it is well-known that the magnetization dynamics can be significantly slowed down by diluting the paramagnetic species in a diamagnetic host,[13,35] the analogue yttrium complex doped with Tb^{III} with a molar ratio of 9:1 was prepared and magnetically investigated. Also in this case no appreciable χ'' was detected, not even under applied static fields (see Figure S15). This observation is in agreement with the large energy separation, or tunnel splitting, of the two lowest-lying states calculated for **Tb**, **Ho**, and **Tm**.

The frequency dependence of the ac susceptibility of **Er** and **Yb**, measured under the application of a static field of 1 kOe, was analyzed using the Casimir-Du Prè formula[36] to take into account a possible distribution of the relaxation times in the Debye model through a phenomenological parameter α (Figure S20). This parameter resulted to be almost zero above 5 K and to increase to 0.2 and 0.3 at 2 K for **Er** and **Yb**, respectively, thus suggesting a relatively narrow distribution. The extracted relaxation times are plotted as a function of temperature in a semi-logarithmic plot (Figure 3). Both **Er** and **Yb** derivatives exhibit an exponential increase of τ on decreasing temperature for the higher investigated temperatures, followed by a gradual leveling of the relaxation time on approaching the lowest investigated temperature. As the linearity of the curve, indicative of the

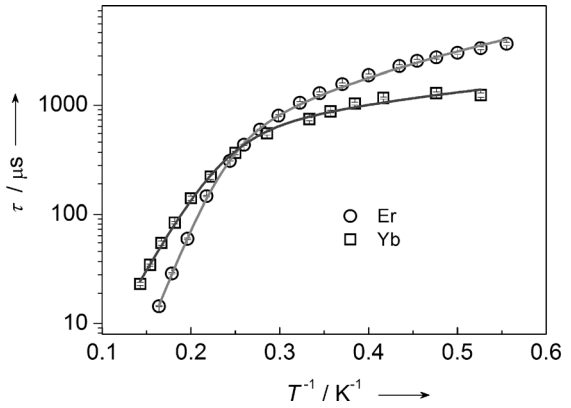

Figure 3. Temperature dependence of the relaxation time (τ in μs) for **Er** and **Yb** derivatives in static field 1000 Oe. The solid lines correspond to the best fit assuming both exponential and power law dependences on T of the relaxation rate.

Arrhenius behavior $\tau = \tau_0 \exp(\Delta/k_B T)$ associated with an Orbach mechanism of relaxation,[2,37] is only observed in a small temperature range, the extracted parameters, $\Delta = 39(2)$ K with $\tau_0 = 2.5(0.8) \times 10^{-8}$ s for **Er** and $\Delta = 29(2)$ K with $\tau_0 = 4(1) \times 10^{-7}$ s for **Yb**, must be considered with caution. To get a better estimation the data were reproduced assuming that the relaxation rate is given by the Orbach contribution, dominating at high temperature, plus an alternative mechanism, the efficiency of which depends on T^n. The best fit curves in Figure 3 were obtained with $\Delta = 49(1)$ K and 35(2) K with $n = 2.5(1)$ and 1.2(1) for **Er** and **Yb**, respectively. The comparison with the calculated splitting given in Table 1 shows an opposite trend for the two ions. Luminescence investigations in the near-infrared region are planned to get an independent estimation of the energy of the first-excited doublets.

The field-induced slow magnetization dynamics of the Er^{III} and Yb^{III} derivatives is quite common among lanthanide complexes. What is more striking here is the absence of any slow dynamics in the other three derivatives. In fact, despite the different shape of the distribution of the electron density all derivatives present easy axis magnetic anisotropy and thus experience a barrier for the reversal of the magnetization. As they have an integer J state their ground doublet is split by transverse anisotropy and states on opposite sides of the barrier are strongly admixed. The oscillatory behavior observed along the series can thus be ascribed to the number of 4f electrons. Spin parity effects on the tunneling efficiency have been observed in polynuclear 3d clusters,[38] and in an isostructural series of single-ion SMMs.[16] However, in the more symmetric series of bis-phthalocyaninate complexes the Tb^{III}, Dy^{III}, and Ho^{III} derivatives show a similar behavior, although with different activation energy.[39]

Summing up, our detailed investigation of six isostructural derivatives of the late lanthanide series and the comparison of their magnetic anisotropy and dynamic behavior allows us to draw some important conclusions.

The proposed correlation between prolate/oblate distribution of electron density and ligand geometry appears to be the driving force in the orientation of the easy axis of magnetization in the series of DOTA complexes. In fact the negative charges of the $DOTA^{4-}$ ligand lie very close to the equatorial plane of the complex as the Ln atom is only at 0.72 Å from the plane formed by the oxygen donor atoms. It is thus expected to favor easy axis anisotropy along the axial direction in case of prolate ions, as indeed observed for Er^{III} and for Yb^{III}. A rational design of the ligand seems therefore the strategy to obtain SMMs of these late lanthanide ions, which are still scarce in the literature.[17,18,20,40,41]

The limits of this simple model are however well-evidenced by our investigation. For oblate ions, like Tb^{III}, Dy^{III} and to a lesser extent Ho^{III}, the axial direction should be a hard one, while the equatorial plane should correspond to an easy plane of magnetization without any barrier for the reversal of the magnetization. This is however neither experimentally observed nor previewed by ab initio calculations, as previously shown for **Dy**, where hydrogen atoms of the apical water molecule are already sufficient to break the axial symmetry of the system and to favor one direction of the equatorial plane.

Our results indicate that easy axis anisotropy is ubiquitous in the late lanthanide series of DOTA complexes but this feature is far to be a sufficient condition to observe slow magnetization dynamics. The uniaxial magnetic anisotropy is, in fact, not correlated with the pseudo-symmetry of the first coordination sphere. In such a situation transverse components of the crystal field play a crucial role and promote efficient under-barrier mechanisms of relaxation, in particular for integer spin states.

The control of the magnetic anisotropy by a rational design of the coordination environment of lanthanide ions, is a relevant topic that goes well beyond the field of molecular magnetism and can only be achieved through sound magneto-structural correlations based on detailed experimental and theoretical studies. A rational ligand design is also of paramount importance to achieve a robust SMM character that persists when lanthanide-based SMMs are employed in spintronic and single-molecule devices.[42]

Experimental Section

The compounds were synthesized following the method previously described,[22] each of them is isostructural to the published structure of $Na[DyDOTA(H_2O)]\cdot 4H_2O$ (see the Supporting Information). Prismatic transparent crystals suitable for X-ray diffraction and for the single-crystal magnetic measurements of Tb^{III}, Er^{III}, and Yb^{III} derivatives were obtained by slow diffusion of acetone in water at room temperature. The static and dynamic magnetic properties are measured on crystalline powders in the Quantum Design MPMS SQUID and in the Quantum Design PPMS equipped with the alternative current measurement option. Crystals glued on a Teflon® cube were indexed by X-ray diffraction on an Oxford X-ray diffractometer and mounted on a horizontal rotating system from Quantum Design for angular dependent magnetometry studies. Luminescence measurements were collected using a Horiba-Jobin Yvon Fluorolog III spectrofluorometer with a F-3018 integrating sphere at 294 K and dedicated N_2 optical dewar at 77 K, under UV irradiation at 380 nm.

Relativistic ab initio calculations were performed for each of the five derivatives. The method used was the CASSCF/CASPT2-RASSI-SO as an implement in the quantum chemistry package MOLCAS

7.4[25] on IBM SP6 supercomputer facility at the Italian computing center CINECA More details are available in the Supporting Information.

Keywords: ab initio calculations · crystal field · lanthanides · luminescence · magnetic properties

[1] G. Christou, D. Gatteschi, D. N. Hendrickson, R. Sessoli, *Mater. Res. Bull.* **2000**, *25*, 66 – 71.

[2] D. Gatteschi, R. Sessoli, J. Villain, *Molecular nanomagnets*, Oxford University Press, Oxford, UK, **2006**.

[3] A. Caneschi, D. Gatteschi, N. Lalioti, C. Sangregorio, R. Sessoli, G. Venturi, A. Vindigni, A. Rettori, M. G. Pini, M. A. Novak, *Angew. Chem.* **2001**, *113*, 1810 – 1813; *Angew. Chem. Int. Ed.* **2001**, *40*, 1760 – 1763.

[4] C. Coulon, H. Miyasaka, R. Clerac, *Single-Molecule Magnets and Related Phenomena*, Springer, Berlin, **2006**, pp. 163 – 206.

[5] N. Ishikawa, M. Sugita, T. Ishikawa, S. Koshihara, Y. Kaizu, *J. Am. Chem. Soc.* **2003**, *125*, 8694 – 8695.

[6] M. A. Al Damen, J. M. Clemente-Juan, E. Coronado, C. Marti-Gastaldo, A. Gaita-Arino, *J. Am. Chem. Soc.* **2008**, *130*, 8874 – 8875.

[7] S.-D. Jiang, B.-W. Wang, G. Su, Z.-M. Wang, S. Gao, *Angew. Chem.* **2010**, *122*, 7610 – 7613; *Angew. Chem. Int. Ed.* **2010**, *49*, 7448 – 7451.

[8] R. A. Layfield, J. J. W. Mcdouall, S. A. Sulway, F. Tuna, D. Collison, R. E. P. Winpenny, *Chem. Eur. J.* **2010**, *16*, 4442 – 4446.

[9] J. D. Rinehart, J. R. Long, *Chem. Sci.* **2011**, *2*, 2078 – 2085.

[10] J. J. Baldoví, S. Cardona-Serra, J. M. Clemente-Juan, E. Coronado, A. Gaita-Ariño, A. Palii, *Inorg. Chem.* **2012**, DOI: ic302068c.

[11] M. Bottrill, L. Kwok, N. J. Long, *Chem. Soc. Rev.* **2006**, *35*, 557 – 571.

[12] L. Armelao, S. Quici, F. Barigelletti, G. Accorsi, G. Bottaro, M. Cavazzini, E. Tondello, *Coord. Chem. Rev.* **2010**, *254*, 487 – 505.

[13] P. E. Car, M. Perfetti, M. Mannini, A. Favre, A. Caneschi, R. Sessoli, *Chem. Commun.* **2011**, *47*, 3751 – 3753.

[14] G. Cucinotta, M. Perfetti, J. Luzon, M. Etienne, P. E. Car, A. Caneschi, G. Calvez, K. Bernot, R. Sessoli, *Angew. Chem.* **2012**, *124*, 1638 – 1642; *Angew. Chem. Int. Ed.* **2012**, *51*, 1606 – 1610.

[15] M. Murugesu, *Nat. Chem.* **2012**, *4*, 347 – 348.

[16] M. Sugita, N. Ishikawa, T. Ishikawa, S.-y. Koshihara, Y. Kaizu, *Inorg. Chem.* **2006**, *45*, 1299 – 1304.

[17] N. Ishikawa, M. Sugita, T. Ishikawa, S. Koshihara, Y. Kaizu, *J. Phys. Chem. B* **2004**, *108*, 11265 – 11271.

[18] H. L. C. Feltham, F. Kloewer, S. A. Cameron, D. S. Larsen, Y. Lan, M. Tropiano, S. Faulkner, A. K. Powell, S. Brooker, *Dalton Trans.* **2011**, *40*, 11425 – 11432.

[19] L. Ungur, L. F. Chibotaru, *Phys. Chem. Chem. Phys.* **2011**, *13*, 20086 – 20090.

[20] M. A. AlDamen, S. Cardona-Serra, J. M. Clemente-Juan, E. Coronado, A. Gaita-Arino, C. Marti-Gastaldo, F. Luis, O. Montero, *Inorg. Chem.* **2009**, *48*, 3467 – 3479.

[21] S.-D. Jiang, S.-S. Liu, L.-N. Zhou, B.-W. Wang, Z.-M. Wang, S. Gao, *Inorg. Chem.* **2012**, *51*, 3079 – 3087.

[22] F. Benetollo, G. Bombieri, S. Aime, M. Botta, *Acta Crystallogr. Sect. C* **1999**, *55*, 353 – 356.

[23] I. J. Hewitt, J. Tang, N. T. Madhu, C. E. Anson, Y. Lan, J. Luzon, M. Etienne, R. Sessoli, A. K. Powell, *Angew. Chem.* **2010**, *122*, 6496 – 6500; *Angew. Chem. Int. Ed.* **2010**, *49*, 6352 – 6356.

[24] J. Luzon, R. Sessoli, *Dalton Trans.* **2012**, *41*, 13556 – 13567.

[25] G. Karlström, R. Lindh, P. A. Malmqvist, B. O. Roos, U. Ryde, V. Veryazov, P. O. Widmark, M. Cossi, B. Schimmelpfennig, P. Neogrady, L. Seijo, *Comput. Mater. Sci.* **2003**, *28*, 222 – 239.

[26] L. F. Chibotaru, L. Ungur, A. Soncini, *Angew. Chem.* **2008**, *120*, 4194 – 4197; *Angew. Chem. Int. Ed.* **2008**, *47*, 4126 – 4129.

[27] P.-H. Guo, J.-L. Liu, Z.-M. Zhang, L. Ungur, L. F. Chibotaru, J.-D. Leng, F.-S. Guo, M.-L. Tong, *Inorg. Chem.* **2012**, *51*, 1233 – 1235.

[28] G. Novitchi, G. Pilet, L. Ungur, V. V. Moshchalkov, W. Wernsdorfer, L. F. Chibotaru, D. Luneau, A. K. Powell, *Chem. Sci.* **2012**, *3*, 1169 – 1176.

[29] F. Tuna, C. A. Smith, M. Bodensteiner, L. Ungur, L. F. Chibotaru, E. J. L. McInnes, R. E. P. Winpenny, D. Collison, R. A. Layfield, *Angew. Chem.* **2012**, *124*, 7082 – 7086; *Angew. Chem. Int. Ed.* **2012**, *51*, 6976 – 6980.

[30] Y.-N. Guo, G.-F. Xu, W. Wernsdorfer, L. Ungur, Y. Guo, J. Tang, H.-J. Zhang, L. F. Chibotaru, A. K. Powell, *J. Am. Chem. Soc.* **2011**, *133*, 11948 – 11951.

[31] H. L. C. Feltham, Y. Lan, F. Kloewer, L. Ungur, L. F. Chibotaru, A. K. Powell, S. Brooker, *Chem. Eur. J.* **2011**, *17*, 4362 – 4365.

[32] K. Bernot, J. Luzon, A. Caneschi, D. Gatteschi, R. Sessoli, L. Bogani, A. Vindigni, A. Rettori, M. G. Pini, *Phys. Rev. B* **2009**, *79*, 134419.

[33] K. Bernot, J. Luzon, L. Bogani, M. Etienne, C. Sangregorio, M. Shanmugam, A. Caneschi, R. Sessoli, D. Gatteschi, *J. Am. Chem. Soc.* **2009**, *131*, 5573 – 5579.

[34] P. A. Malmqvist, B. O. Roos, B. Schimmelpfennig, *Chem. Phys. Lett.* **2002**, *357*, 230 – 240.

[35] F. Luis, M. J. Martìnez- Peréz, O. Montero, E. Coronado, S. Cardona-Serra, C. Martì-Gastaldo, J. M. Clemente-Juan, J. Ses, D. Drung, T. Schurig, *Phys. Rev. B* **2010**, *82*, 060403.

[36] H. B. J. Casimir, F. K. Duprè, *Physica* **1938**, *5*, 507.

[37] A. Abragam, B. Bleaney, *Electron Paramagnetic Resonance of Transition Ions*, Dover, New York, **1986**.

[38] W. Wernsdorfer, N. E. Chakov, G. Christou, *Phys. Rev. Lett.* **2005**, *95*, 037203.

[39] N. Ishikawa, *Polyhedron* **2007**, *26*, 2147 – 2153.

[40] J.-L. Liu, K. Yuan, J.-D. Leng, L. Ungur, W. Wernsdorfer, F.-S. Guo, L. F. Chibotaru, M.-L. Tong, *Inorg. Chem.* **2012**, *15*, 8538 – 8544.

[41] P.-H. Lin, W.-B. Sun, Y.-M. Tian, P.-F. Yan, L. Ungur, L. F. Chibotaru, M. Murugesu, *Dalton Trans.* **2012**, *41*, 12349 – 12352.

[42] a) M. Urdampilleta, S. Klyatskaya, J. P. Cleuziou, M. Ruben, W. Wernsdorfer, *Nat. Mater.* **2011**, *10*, 502 – 506; b) R. Vincent, S. Klyatskaya, M. Ruben, W. Wernsdorfer, F. Balestro, *Nature* **2012**, *488*, 357 – 360.